Biogeosciences Discuss., 4, 4443–4458, 2007
www.biogeosciences-discuss.net/4/4443/2007/

Biogeosciences Discussions

Biogeosciences Discussions is the access reviewed discussion forum of *Biogeosciences*

Miniaturized biosignature analysis reveals implications for the formation of cold seep carbonates at Hydrate Ridge (off Oregon, USA)

T. Leefmann[1], J. Bauermeister[1], A. Kronz[1], V. Liebetrau[2], J. Reitner[1], and V. Thiel[1]

[1]Geoscience Centre (GZG), University of Göttingen, Göttingen, Germany
[2]Leibniz-Institut für Meereswissenschaften (IfM-GEOMAR), Kiel, Germany

Received: 9 November 2007 – Accepted: 16 November 2007 – Published: 28 November 2007

Correspondence to: V. Thiel (vthiel@gwdg.de)

Abstract

Methane-related carbonates from Hydrate Ridge typically show several macroscopically distinguishable phases, namely whitish aragonite, lucent aragonite, and gray micrite. The relationship of these phases to particular microorganisms or biogeochemical processes is as yet unclear. We used a miniaturized biomarker technique on mg samples, combined with factor analysis and subsequent electron microprobe analysis, to study lipid biomarkers and chemical compositions of the individual phases. This allows us to identify particular mechanisms involved in the formation of the different carbonate precipitates. Our combined analysis of biomarkers and petrographic traits shows that most of the lipids related to the anaerobic oxidation of methane (>90% by weight) are concentrated within only a minor compartment (~20% by volume) of the Hydrate Ridge carbonates (whitish aragonite). The patterns indicate that the whitish aragonite represents fossilized biofilms of methanotrophic consortia, whereas the precipitation of the lucent aragonite does not seem to be directly controlled by microorganisms. The gray micrite shows a partly Mg-calcitic mineralogy, higher pyrite contents, and a much higher proportion of allochthonous biomarkers. The formation of these precipitates is interpreted to reflect periodic methane-rich fluid pulses that disrupted the sediments and promoted the growth of the respective methanotrophic consortia along fluid pathways.

1 Introduction

Specific carbonates occur at cold seep sites, where methane-rich fluids are leaking from the seafloor. These "seep carbonates" typically show highly negative $\delta^{13}C$ values (Greinert et al., 2001) indicating that they formed from bicarbonate produced by anaerobic oxidation of methane (AOM; Ritger et al., 1987). AOM is mediated by a consortia of methanotrophic archaea and sulphate-reducing bacteria (SRB), which have been characterized by 16S rRNA investigations (Hinrichs et al., 1999; Boetius et al., 2000).

BGD

4, 4443–4458, 2007

Two major phylogenetic groups of methanotrophic archaea (ANME-1 and ANME-2, ANME=anaerobic methane oxidizers) were distinguished. While ANME-2 archaea have been observed in tight association with SRB of the Desulfosarcina/Desulfococcus group, ANME-1 archaea sometimes occur with these SRB, but at other times are observed as monospecific aggregations or isolated filaments (Orphan et al., 2002). In anoxic marine sediments, carbonate crusts, and recent microbial mats from cold seep sites, methanotrophic consortia can be traced using specific, strongly ^{13}C-depleted biomarkers. Different species of methanotrophic archaea are considered to be the sources of characteristic isoprenoids (Hinrichs et al., 1999; Elvert et al, 2005; Blumenberg et al., 2004; Pape et al., 2005). These isoprenoids include C_{20} and C_{25} irregular isoprenoid hydrocarbons (crocetane and 2,6,10,15,19-pentamethylicosane and unsaturated derivatives), the glycerol diethers archaeol and *sn*-2-hydroxyarchaeol (2,3-di-O-phytanyl-*sn*-glycerol and 2-O-3-hydroxyphytanyl-3-O-phytanyl-*sn*-glycerol), and glycerol dialkyl glycerol tetraethers (GDGT) carrying two C_{40} isopranyl moieties. Non-isoprenoid monoalkylglycerolethers (MAGEs), 1,2-dialkylglycerolethers (DAGEs), and C_{14} to C_{18} *n*-, *iso*- and *anteiso*-fatty acids, and alcohols found at cold-seeps have commonly been regarded as biomarkers for associated SRB (Pancost et al., 2001a; Hinrichs et al., 2000).

The cold seep sites at Hydrate Ridge, located about 90 km off the coast of Oregon (USA) at 600 m to 800 m water depth, have been extensively studied since the mid-1980s. Different seep carbonate lithologies have been the targets of several investigations (Kulm and Suess, 1990; Ritger et al., 1987; Bohrmann et al., 1998; Greinert et al., 2001). Generally, authigenic carbonates from Hydrate Ridge consist primarily of aragonite (Greinert et al., 2001). At SE-Knoll, an up to 90 m high chemoherm located about 15 km SE from the southern summit of Hydrate Ridge (Bohrmann et al, 2000), three major carbonate types are closely interfingered. These types consist of (i) a macroscopically opaque, cryptocrystalline variety ranging in color from white to pinkish and brownish, (ii) a translucent aragonite consisting of fibrous, acicular crystals, and (iii) a gray, microcrystalline carbonate with varying content of Mg-calcite and

various components, namely shell fragments, pellets containing pyrite, peloids and detrital quartz, and feldspar grains (Teichert et al., 2005).

In order to study the linkage of these phases to particular microorganisms and/or biogeochemical processes, we used a miniaturized biomarker technique, combined with factor analysis, and subsequent electron microprobe analyses. The aim was to identify differences in the lipid biomarker patterns and the chemical compositions between the phases that would allow us to understand the mechanisms involved in forming the particular carbonate precipitates.

2 Material and methods

Sample collection – The samples were obtained from a carbonate block collected during cruise SO165/2 of RV "Sonne" in August 2002. The block was gathered directly from the top of the SE-Knoll chemoherm using a TV grab (Station 230-1, TVG-13, 44° 27.04′ N, 125° 01.80′ W, 615 m water depth). First U-Th isotope analyses of 5 subsamples from this core, using the MC-ICP-MS method after Fietzke et al. (2005), imply distinct precipitation phases of cold-seep related carbonates between 205 and 98 ka BP (unpublished).

Sample preparation – From a 28.5 cm (length) by 50 mm (diameter) core drilled from sample TVG 13, 18 micro drill cores (<2 mm long, 2 mm in diameter, 6–21 mg in weight) were taken using a diamond-studded hollow drill. Microscope observations allowed us to classify the micro-drill cores into three distinct phases according to Teichert et al. (2005): (i) "whitish aragonite" (8 samples), (ii) "lucent aragonite" (6 samples), and (iii) "gray micrite" (4 samples). The samples were pestled and extracted in screwed glass vials using 200 μL CH_2Cl_2 and ultrasonication (35 min; 60°C). After centrifuging, the supernatant was decanted. The extraction was repeated twice. The combined extracts were dried, and derivatized by adding 50 μL N,O-bis (trimethylsilyl)trifluoroacetamide (BSTFA; 90 min; 80°C). The reaction mixtures were dried in a gentle stream of nitrogen, and redissolved in *n*-hexane. For each mg of the weighted carbonate sample,

BGD
4, 4443–4458, 2007

EGU

2 μL of *n*-hexane were added. 1 μL of each extract was analyzed in a coupled gas chromatograph mass spectrometer (GC/MS).

GC/MS – The GC/MS system used was a Varian CP-3800 GC coupled to a Varian 1200 quadrupole MS operated in electron impact mode at 70 eV. The samples were injected on-column into a fused silica capillary column (Phenomenex ZB-1; 30 m; 0.25 mm; 0.1 μm film thickness). In the injector, the samples were heated from 50°C (0.2 min isothermal) to 290°C at 150°C/min (5 min isothermal). The GC-oven was programmed from 50°C (1 min isothermal) to 300°C at 10°C/min, and was held at 300°C for 15 min. Helium was used as the carrier gas at a flow rate of 1.4 mL. Compounds were identified by comparison with published mass spectral data.

Factor analysis – A factor analysis was implemented using Statistica 6.0, developed by Statsoft Inc, Tulsa. The compound concentrations were treated as multivariate to show correlations of the compounds with each other (biomarker families). Absolute concentrations (in μg/g carbonate weighted samples) were used as base data. Factors were extracted by Principle Component Analyses (PCA). The maximum number of factors to be extracted was determined using the scree test (Cattel, 1966a). The rotational strategy was varimax normalized (Kaiser, 1958, 1959).

Electron microprobe analysis – Polished thin sections (250 μm thickness) were prepared from sampled areas of the carbonate. Element distributions of Mg, S, Mn, Fe, Sr, (wavelength dispersive system) and Ca (energy dispersive system) were mapped using a JEOL JXA 8900 RL electron microprobe. The acceleration voltage was set to 15 kV and a beam current of 40 nA, measured by Faraday cup, was used. The acquisition time was set to 70 ms per step. The scan grid was spaced at 20 or 40 μm steps, depending on the dimension of each area, resulting in total dimensions between 7×5 and 10×20 mm. The backscatter signal in composition mode and the cathodoluminescence signal (integrated spectral range from 200 to 900 nm) were acquired simultaneously. Since carbonates have sensitive behavior under electron bombardment, the beam diameter was set to 20 μm.

3 Results

Biomarkers – The whitish aragonite samples showed the highest lipid biomarker concentrations, containing more than 90% of the total AOM-related lipid signature observed (Table 1, Fig. 1). In all whitish aragonite samples (n=8), archaeol, *sn*-2-hydroxyarchaeol and DAGEs were the most prominent lipid biomarkers (Table 1). In five out of eight samples, *sn*-2-hydroxyarchaeol was more abundant than archaeol. The most abundant DAGE showed n-C_{14} and C_{17}-cyclopropyl moieties at the *sn*-1 and *sn*-2 positions, respectively (DAGE IIa according to the designation given by Pancost et al., 2001a). Another, somewhat less abundant, DAGE containing two *anteiso*-C_{15} alkyl chains was observed in the whitish aragonite samples (DAGE If according to Pancost et al., 2001a). Other DAGEs occurred in trace concentrations. Furthermore, crocetane, PMI, and phytanol occurred in all whitish aragonite samples, but with concentrations about an order of magnitude lower than those of the ether lipids (Table 1).

Unlike the whitish aragonite, the lucent aragonite samples (n=6) contained only trace amounts of lipid biomarkers (Table 1). n-alkanes (n-C_{23} to n-C_{31}), n-fatty acids (n-C_{14} to n-C_{18}), squalene, and sterols, specifically cholesterol and sitosterol, dominate the patterns. In two out of six samples, PMI was detected, whereas phytanol and *sn*-2-hydroxyarchaeol were observed in only one sample each. Archaeol was found in three samples, while crocetane and DAGEs were generally below the detection limit in the lucent aragonite (Table 1).

The gray micrite samples (n=4) were characterized by archaeol as the main compound, although its absolute concentrations were an order of magnitude lower than in the whitish aragonite (Table 1). Notably, *sn*-2-hydroxyarchaeol was completely absent from the gray micrite, whereas smaller amounts of DAGEs, PMI, crocetane, sterols, n-fatty acids, and trace-amounts of n-alkanes were evident. Average concentrations of sterols and n-fatty acids were even higher in the gray micrite than in the whitish aragonite, except for n-C_{18}, which was similarly abundant in both phases. A specific trait of the gray micrite was the occurrence of perylene, which was found in three of the four

samples analyzed.

Factor analysis – The two factors extracted accounted for 44.9% and 24.6% of the total variance. The factor loadings plot revealed a compound group consisting of PMI, crocetane, DAGE IIa, DAGE If, archaeol, *sn*2-hydroxyarchaeol, and phytanol, which has slightly negative loadings with factor 1 and highly positive loadings with factor 2 (Fig. 2). A second group of compounds that loads positive with factor 1 and slightly negative with factor 2 included *n*-alkanes, *n*-fatty acids, and sterols. One compound, *n*-tricosane (*n*-C_{23}), plotted between the two compound groups.

Electron microprobe analyses – The electron microprobe data showed that the whitish aragonite was considerably enriched in Sr compared to the lucent aragonite (Fig. 3h). Both aragonite phases nevertheless revealed higher Sr concentrations than the gray micrite (Fig. 3f). Ca was somewhat more abundant in the lucent aragonite than in the whitish aragonite and the gray micrite; Mn was not observed in any of the phases. Fe, Mg, and S were detected in the gray micrite, but they were below detection limit in the aragonites. In the gray micrite, distributions of Mg and Ca were anticorrelating (Fig. 3c, e). S and Fe, on the other hand, spatially correlated (Fig. 3b, d).

4 Discussion

The strong correlation between the concentrations of PMI, crocetane, DAGE IIa, DAGE If, archaeol, and *sn*-2-hydroxyarchaeol suggests that these AOM-related biomarkers originate from a closely associated biological source. Blumenberg et al. (2004) proposed high proportions of *sn*-2-hydroxyarchaeol vs. archaeol, and the presence of crocetane, as traits to distinguish microbial consortia dominated by ANME-2 vs. ANME-1. Concentrations of these compounds are highest in the whitish aragonite. Here, the *sn*-2-hydroxyarchaeol/archaeol ratios range from 0.48 to 2.13 (Table 1). This spread can be interpreted in terms of varying contributions of ANME-1 vs. ANME-2 archaea, respectively, which were both observed in sediments from Hydrate Ridge (Elvert et al., 2005; Knittel et al., 2003). However, unlike archaeol, *sn*-2-hydroxyarchaeol is rarely

present in the fossil record (Peckmann and Thiel, 2004), indicating its preferential diagenetic degradation, or even conversion to archaeol by dehydroxylation of the phytyl moiety. Therefore, the ratios of *sn*-2-hydroxyarchaeol/archaeol of Hydrate Ridge material must be interpreted cautiously, especially when comparing with data from recent microbial consortia. As the studied carbonates are several ten thousand years old, the original abundance of *sn*-2-hydroxyarchaeol may have been considerably higher than it is now. Furthermore, taking into account the prominent occurrence of crocetane found exclusively in whitish aragonite samples (Table 1), we propose that ANME-2 archaea were directly involved in forming this carbonate type.

High abundances of DAGEs with non-isoprenoid alkyl moieties have been assigned to the SRB present in the methanotrophic consortia (Pancost et al., 2001a), due to their structural similarity to ether lipids of some deeply branching bacteria. Here, we follow this commonly accepted interpretation. However, it should be pointed out that the bacterial origin of DAGEs was recently challenged: Elvert et al. (2005) observed high abundances of these compounds in sections of a Hydrate Ridge sediment core where ANME-1 dominated while the numbers of SRB-cells were markedly low. Although the exact source organisms in these systems are as yet unclear, the high abundances of DAGEs in the whitish aragonite and the strong correlation with archaeal isoprenoid biomarkers clearly imply an origin from within the consortia involved in AOM.

The traces of lipid biomarkers in the lucent aragonite did not show any specific pattern (Fig. 1). Considering (i) the low sample amounts used, (ii) the low compound concentrations, and (iii) the absence of a characteristic biomarker pattern, contamination from the other carbonate phases during sample preparation is a conceivable source for the lipids observed in the lucent aragonite samples. Thus, it seems unlikely that there is direct involvement of particular AOM-related (and other) microorganisms in the precipitation of the lucent aragonite, as proposed for the whitish aragonite.

In the gray micrite, abundant Mg reflects a partly Mg-calcitic mineralogy, corresponding to micrites described at another SE-Knoll location (Teichert et al., 2005). Furthermore, the similarity of distributions of Fe and S in the gray micrite indicates likely

pyrite occurrence in these carbonates (Fig. 3b, d; see also Teichert et al., 2005). The gray micrite contained biomarker compounds from both compound clusters revealed by factor analysis (Fig. 2). The presence of PMI, archaeol, and DAGEs, together with the conspicuous absence of *sn*-2-hydroxyarchaeol and the very low amounts of crocetane, suggests that ANME-1 archaea are involved in the formation of the gray micrite, rather than ANME-2 archaea. On the other hand, factor analysis suggests that long-chain *n*-alkanes, conventional sterols (sitosterol, cholesterol), and *n*-fatty acids represent water-column-sourced contributions rather than AOM-derived compounds. In this context, it is interesting that the intermediate position of *n*-tricosane between the two compound clusters (Fig. 2) corresponds with a dual, partly AOM-related origin of this hydrocarbon (Thiel et al., 2001). Perylene, which is thought to originate from both terrestrial and aquatic organic matter during diagenesis (Silliman et al., 2000), is presumably derived from allochthonous sources. These combined findings are interpreted to reflect incorporation of allochthonous organic and inorganic matter during AOM-induced carbonate precipitation resulting in the formation of the gray micrite.

5 Conclusions

Combining miniaturized lipid biomarker analysis and electron microprobe analysis allowed us to resolve biosignatures of a complex microbialite at the mm-scale, and allowed us to develop a model for the origin of distinct carbonate phases. The results showed a highly localized distribution of lipid biomarkers within the Hydrate Ridge carbonates. More than 90% of the AOM-related lipid signature was concentrated in only about 20% of the total carbonate rock volume, specifically in a whitish aragonite phase. The biomarker and inorganic patterns of the whitish aragonite were highly specific and indicated an association with methanotrophic consortia containing ANME-2 archaea and sulfate-reducing bacteria. We suggest that the whitish aragonite formed during periodic methane-rich fluid pulses that disrupted the sediment and led to the growth of the respective microorganisms along fluid pathways. By contrast, low amounts of

lipid-biomarkers and lower Sr-contents observed in the lucent aragonite indicated that the formation of this precipitate was not directly mediated by microorganisms, but rather occurred during intermittent periods of low fluid supply. The gray micrite showed both authigenic and allochthonous signals that likely originated from carbonate cementation of allochthonous organic and inorganic matter caused by microbial anaerobic methanotrophy during phases of low background methane supply.

Acknowledgements. We are grateful to P. Linke and C. Utecht (IFM-GEOMAR, The Leibniz Institute of Marine Sciences at the University of Kiel), who coordinated the joint project COMET (COntrols on METhane fluxes and their climatic relevance in marine gas hydrate-bearing sediments), and A. Eisenhauer (IFM-GEOMAR), chief scientist of RV "Sonne" cruise 165/2, which retrieved the carbonates studied here. We further wish to thank K. Simon (University of Göttingen) for an introduction to factor analysis. This study was financially supported by the German Ministry of Education and Research (BMBF) (Grant 03G0600D, COMET), and by the Deutsche Forschungsgemeinschaft (Grant Th 713/3). This is publication no. GEOTECH–294 of the R and D-Programme GEOTECHNOLOGIEN.

References

Blumenberg, M., Seifert, R., Reitner, J., Pape, T., and Michaelis, W.: Membrane lipid patterns typify distinct anaerobic methanotrophic consortia, P. Natl. Acad. Sci. USA, 101, 11 111–11 116, 2004.

Boetius, A., Ravenschlag, K., Schubert, C., Rickert, D., Widdel, F., Gieseke, A., Amann, R., Jørgensen, B. B., Witte, U., and Pfannkuche, O.: A marine microbial consortium apparently mediating anaerobic oxidation of methane, Nature, 407, 623–626, 2000.

Bohrmann, G., Linke, P., Suess, E., and Pfannkuche, O.: FS SONNE Cruise Report SO143, GEOMAR Rep. 93, 243 pp., 2000.

Bohrmann, G., Greinert, J., Suess, E., and Torres, M.: Authigenic carbonates from the Cascadia subduction zone and their relation to gas hydrate stability, Geology, 26, 647–650, 1998.

Cattell, R. B.: The scree test for the number of factors. Multivar. Behav. Res., 1, 245–276, 1966a.

Elvert M., Hopmans, E. C., Treude, T., Boetius, A., and Suess, E.: Spatial variations of methanotrophic consortia at cold methane seeps: implications from a high-resolution molecular and isotopic approach, Geobiology, 3, 195–209, 2005.

Fietzke, J., Liebetrau, V., Eisenhauer, A., and Dullo, C.: Determination of uranium isotope ratios by multi-static MIC-ICP-MS: method and implementation for precise U- and Th-series isotope measurements, J. Anal. Atom. Spectrom., 20, 395–401, 2005.

Greinert, J., Bohrmann, G., and Suess, E.: Gas hydrate-associated carbonates and methane-venting at Hydrate Ridge: classification, distribution, and origin of authigenic lithologies, in: Natural Gas Hydrates: Occurrence, Distribution, and Detection, edited by: Paull, C. K. and Dillon, W. P., American Geophysical Union, Washington, DC, USA, 99–113, 2001.

Hinrichs, K.-U., Hayes, J. M., Sylva, S. P., Brewer, P. G., and DeLong, E. F.: Methane-consuming archaebacteria in marine sediments, Nature, 398, 802–805, 1999.

Hinrichs, K.-U., Summons, R. E., Orphan, V., Sylva, S. P., and Hayes, J. M.: Molecular and isotopic analyses of anaerobic methane-oxidizing communities in marine sediments, Org. Geochem., 31, 1685–1701, 2000.

Kaiser, H. F.: The varimax criterion for analytic rotation in factor analyses, Psychometrika, 23, 187–200, 1958.

Kaiser, H. F.: The application of electronic computers to factor analysis, Educ. Psychol. Meas., 19, 141–151, 1959.

Knittel, K., Boetius, A., Lemke, A., Eilers, H., Lochte, K., Pfannkuche, O., Linke, P., and Amann, R.: Activity, distribution, and diversity of sulfate reducers and other bacteria in sediments above gashydrate (Cascadia margin, Oregon), Geomicrobiol. J., 20, 269–294, 2003.

Kulm, L. D. and Suess, E.: Relationship between carbonate deposits and fluid venting: Oregon accretionary prism, J. Geophys. Res., 95, 8899–8915, 1990.

Orphan, V. J., House, C. H., Hinrichs, K.-U., McKeegan, K. D., and DeLong, E. F.: Multiple archaeal goups mediate methane oxidation in anoxic cold seep sediments, P. Natl. Acad. Sci. USA, 99, 7663–7668, 2002.

Pape T., Blumenberg M., Seifert R., Gulin S.B., Egorov V. N., and Michaelis W.: Lipid geochemistry of methane-derived Black Sea carbonates, Palaeogeogr. Palaeocl., 227, 31–47, 2005.

Pancost, R. D., Bouloubassi, I., Aloisi, G., Sinninghe Damsté, J. S., and the Medinaut Shipboard Scientific Party: Three series of non-isoprenoid dialkyl glycerol diethers in cold-seep carbonate crusts, Org. Geochem., 32, 695–707, 2001a.

Peckmann, J. and Thiel, V.: Carbon cycling at ancient methane-seeps, Chem. Geol., 205, 433–467, 2004.

Ritger, S., Carson, B., and Suess, E.: Methane-derived authigenic carbonates formed by subduction-induced pore-water expulsion along the Oregon/Washington margin, Geol. Soc. Am. Bull., 98, 147–156, 1987.

Silliman, J. E., Meyers, P. A., Ostrom, P. H., Ostrom, N. E., and Eadie, B. J.: Insights into the origin of perylene of sediments from Saanich Inlet, British Columbia, Org. Geochem., 31, 1133–1142, 2000.

Teichert, B. M. A., Bohrmann, G., and Suess, E.: Chemoherms on Hydrate Ridge – Unique microbially-mediated carbonate build-ups growing into the water column, Palaeogeogr. Palaeocl., 227, 67–85, 2005.

Thiel, V., Peckmann, J., Schmale, O., Reitner, J., and Michaelis, W.: A new straight-chain hydrocarbon biomarker associated with anaerobic methane cycling, Org. Geochem., 32, 1019–1023, 2001.

Table 1. Concentrations of lipid biomarkers (μg/g of rock; *n*-C_X=saturated *n*-alkane containing X carbon atoms, *n*-$C_X$fa saturated *n*-fatty acid containing X carbon atoms, n. d.=not detected)

	whitish aragonite (I) samples ($\mu g\,g^{-1}$ rock)								lucent aragonite (II) samples ($\mu g\,g^{-1}$ rock)						gray micrite (III) samples ($\mu g\,g^{-1}$ rock)			
sample	1r1	3	7	7r1	9a	9b	9c	9d	2	2r1	2r2	8a	8b	8c	6r1	10r1	10r3	11r1
crocetane	0,04	0,05	0,70	0,77	0,46	0,07	0,06	0,07	<0,01	n. d.	n. d.	n. d.	n. d.	n. d.	0,04	0,03	0,09	0,06
PMI	0,29	0,34	0,47	1,00	1,07	0,14	0,16	0,09	0,07	0,14	n. d.	n. d.	n. d.	n. d.	0,02	0,15	0,28	0,22
n-C_{23}	0,02	0,02	n. d.	0,02	0,01	0,01	0,01	n. d.	0,02	0,02	0,03	n.'d.	n. d.	0,08	0,02	0,01	0,02	n. d.
n-C_{27}	0,01	0,01	n. d.	n. d.	0,01	n. d.	n. d.	n. d.	0,03	0,06	0,06	0,01	n. d.	0,02	0,03	0,01	n. d.	0,01
n-C_{28}	0,01	0,01	n. d.	<0, 01	0,01	n. d.	0,01	n. d.	0,02	n. d.	0,06	0,01	n. d.	0,02	0,03	<0, 01	0,01	0,01
n-C_{29}	0,03	0,02	n. d.	0,01	0,01	n. d.	n. d.	n. d.	0,01	0,05	0,06	0,02	0,01	0,01	0,05	<0, 01	0,02	0,01
n-C_{30}	n. d.	0,01	n. d.	n. d.	n. d.	n. d.	n. d.	n. d.	n. d.	n. d.	0,08	0,02	n. d.	n. d.	0,02	n. d.	n. d.	n. d.
n-C_{31}	0,02	0,02	n. d.	0,01	0,01	n. d.	n. d.	n. d.	n. d.	0,01	0,05	0,02	n.d.	0,01	0,05	0,01	0,01	0,01
perylene	n. d.	n. d.	n. d.	n. d.	n. d.	n. d.	n. d.	n. d.	n. d.	n. d.	n. d.	n. d.	n. d.	n. d.	0,01	0,03	0,16	n.d.
phytanol	0,77	0,16	0,35	0,25	0,27	0,06	0,09	0,25	0,04	0,10	n. d.	n. d.	0,14	n. d.	0,01	0,03	0,08	0,16
sitosterol	n. d.	0,06	0,07	n. d.	0,09	0,04	0,03	0,07	0,07	0,10	0,17	0,05	0,02	0,04	0,13	0,04	0,06	0,04
cholesterol	0,15	0,12	0,06	n. d.	0,09	0,10	0,03	0,31	0,08	0,10	0,30	0,12	0,05	0,05	0,20	0,10	0,17	0,16
DAGE IIa	0,12	1,89	2,61	5,96	6,19	0,20	0,83	0,40	n. d.	0,06	n. d.	n. d.	n. d.	n. d.	0,02	0,08	0,29	0,19
DAGE If	0,32	0,50	1,08	0,66	0,53	0,02	0,08	n. d.	n. d.	n. d.	n. d.	n. d.	n. d.	n. d.	0,24	0,01	0,07	0,06
archaeol	4,62	1,86	4,64	9,77	10,46	0,39	0,93	0,43	0,16	0,31	n. d.	0,12	n. d.	n. d.	0,06	0,19	0,68	0,73
sn-2-hydroxy archaeol	4,64	0,02	6,80	20,81	6,21	0,47	0,44	0,71	n. d.	0,16	n. d.	n. d.	n. d.	n. d.	n. d.	n. d.	n. d.	n. d.
n-C_{14}fa	0,02	0,02	n.d.	0,01	<0, 01	n.d.	0,02	0,07	0,03	0,05	0,07	0,01	0,02	0,01	0,08	0,02	0,03	0,02
n-C_{16}fa	0,06	0,10	0,06	0,03	0,15	0,08	0,06	0,04	0,13	0,10	0,25	0,08	0,04	0,06	0,26	0,06	0,08	0,08
n-C_{18}fa	0,04	0,05	0,09	0,03	0,10	0,05	0,03	0,17	0,04	0,07	0,18	0,06	0,02	0,05	0,14	0,03	0,05	0,04
sn-2-hydroxarchaeol/ archaeol ratio	1,01	0,01	1,47	2,13	0,59	1,18	0,48	1,64	–	0,52	–	–	–	–	–	–	–	–

BGD
4, 4443–4458, 2007

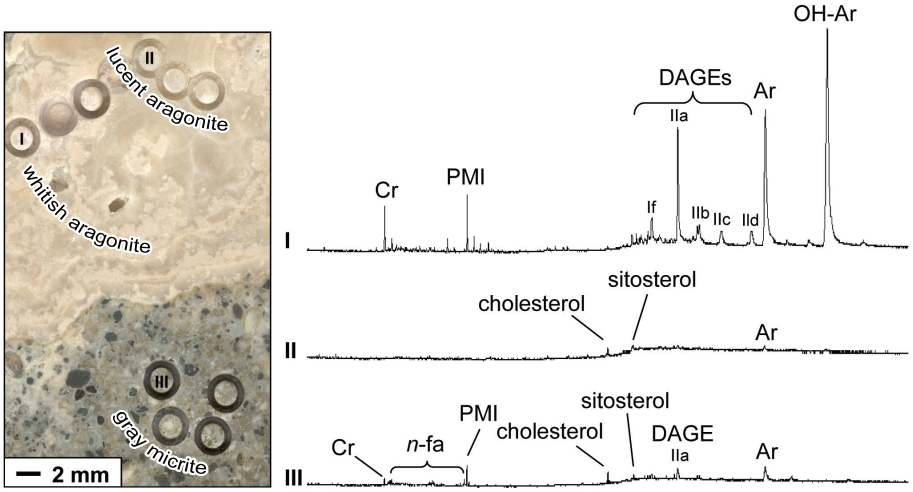

Fig. 1. Enlarged image of area III (see Fig. 3) sampled for lipid biomarker analyses (left) and total ion currents (right) of individual micro-drill cores. (I) whitish aragonite; (II) lucent aragonite; (III) gray micrite. Cr=crocetane, Ar=archaeol, OH-Ar=*sn*-2-hydroxyarchaeol; DAGE If, IIa, IIb, IIc, IId (abbreviations according to Pancost et al., 2001a); *n*-fa=*n*-fatty acids).

BGD
4, 4443–4458, 2007

EGU

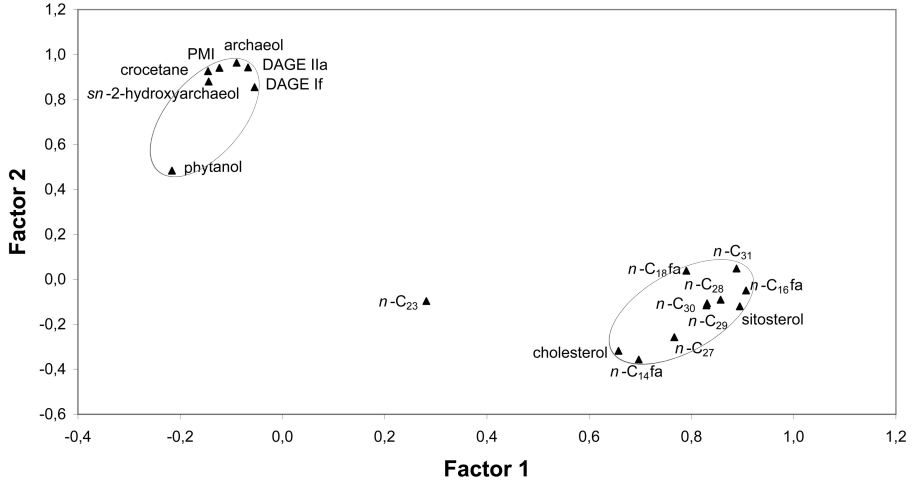

Fig. 2. Two-dimensional plot of compound factor loadings, showing two distinct groups of lipid biomarkers (marked by gray ellipses) (n-C_X=saturated n-alkane containing X carbon atoms, n-$C_X$fa=saturated n-fatty acid containing X carbon atoms).

BGD
4, 4443–4458, 2007

EGU

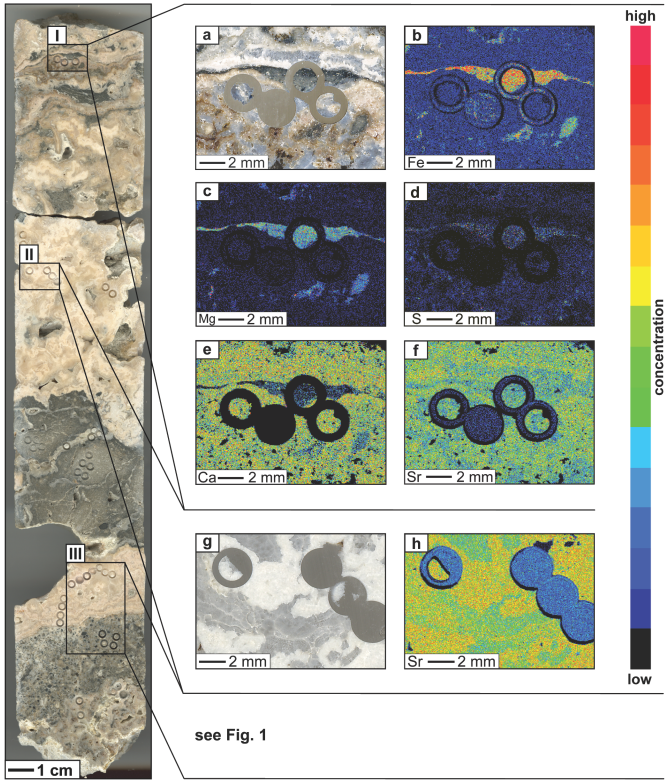

Fig. 3. Cross-section of the sampled drill core with areas I, II, and III (marked by black frames) analyzed by electron microprobe and/or sampled for miniaturized biomarker analyses. **(a)** reflected light image of thin section area I showing layer of gray micrite surrounded by a pinkish variety of whitish aragonite. **(b)** element map showing Fe distribution of area I. **(c)** element map showing Mg distribution of area I. **(d)** element map showing S distribution of area I. **(e)** element map showing Ca distribution of area I. **(f)** element map showing Sr distribution of area I. **(g)** reflected light image of thin section area II showing lucent and whitish aragonite. **(h)** element map showing Sr distribution of area II.

BGD
4, 4443–4458, 2007

EGU